Seasonal Changes of Sea Ice Thickness in the Eastern Arctic Ocean Evident from Remotely Sensed and In-Situ Observations in 2013–2015

Andrey V. Pnyushkov *

Posted Date: 2 August 2023

doi: 10.20944/preprints202308.0112.v1

Keywords: sea ice thickness; Arctic Ocean; Eurasian Basin; ice profiling sonars

Article

Seasonal Changes of Sea Ice Thickness in the Eastern Arctic Ocean Evident from Remotely Sensed and In-Situ Observations in 2013–2015

Andrey V. Pnyushkov

International Arctic Research Center, University of Alaska Fairbanks, 2160 Koyukuk Drive, Fairbanks, AK, 99775, USA; avpnyushkov@alaska.edu

Abstract: The study focuses on conducting a quantitative comparison of sea ice thickness data obtained through satellite-based remote sensing and in-situ observations in the eastern Arctic Ocean from September 2013 to September 2015 as part of the Nansen and Amundsen Basins Observational System (NABOS) program. Upward-looking sonar observations from an oceanographic mooring at the northern slope of the Laptev Sea (78°25'N, 125°04'E) were used for comparing instrumental measurements of ice thickness with data from the remotely sensed CryoSat-2 and CryoSat2/SMOS datasets. The comparison results indicate a significant tendency for satellite products to overestimate sea ice thickness by more than 40 cm, particularly for moderate and thick ice conditions. Caution is advised when using these satellite-based measurements. Sea ice ridging is identified as one of the possible factors contributing to the observed discrepancy. The continental slope of the Laptev Sea experienced a prevalence of ridged ice over level ice during the period from 2013 to 2015. In the spring season (March-May), ridged ice was observed approximately 60% of the time, while level ice was observed around 40% of the time. However, the most significant relative contribution of ridging to ice thickness was observed during the initial ice formation period (from October through December) when sea ice is thin (<1 m). During these months, the relative difference between the mean and modal ice thickness, which reflects the mean variation between the deformed and thermodynamically grown level sea ice, could be as high as 70%.

Keywords: sea ice thickness; Arctic Ocean; Eurasian Basin; ice profiling sonars

1. Introduction

Arctic sea ice plays an essential role in the global climate system, serving as a key indicator of thermal changes at high latitudes driven by global climate changes and the ongoing Atlantification of the Arctic Ocean [1–3]. Over the past few decades, the Arctic Ocean's sea-ice cover has undergone significant transformations, particularly noticeable in the reduction of multi-year ice thickness, spatial extent, and total volume (e.g., [4]). However, the rate of these changes and their regional variations remain uncertain and subject to ongoing debate. For instance, a study by Kwok and Rothrock [5], which combined in-situ and remotely sensed ice records, indicated a decrease of 1.75 m in mean winter ice thickness since 1980, with the most rapid decline (about 0.2 m per year) occurring during the last five years of the records analyzed. Nevertheless, more recent estimates over a shorter period (2011-2018) covered by the CryoSat-2 (CS-2) satellite mission observations suggested smaller rates of ice thickness reduction, with the mean ice thickness decreasing by up to 2 m [6].

The notable sea-ice loss observed during the record-breaking years of 2007 and 2012 was primarily concentrated in the Canadian sector of the Arctic Ocean. However, in more recent years (2013-2022), significant sea-ice decline has also been evident in the eastern Eurasian Basin (EB) sector of the Arctic. This decline exhibited comparable or even greater magnitude compared to that observed in the Canadian Basin. While satellite observations provide a reasonably good assessment of sea ice area and extent, the validation against in-situ measurements for ice thickness in the eastern

 doi:10.20944/preprints202308.0112.v1

EB remains insufficient [1], leading to considerable uncertainty in the rates of ice thickness decline for this region.

In climate research, satellite measurements, along with mathematical models, are essential tools for obtaining reliable information about changes in the thickness of the ice cover across the entire Arctic Ocean. These measurements serve as a crucial source of data, given the vast scale of the region, providing valuable insights into climate-related variations in sea ice thickness. Therefore, the main objective of this study is to offer readers an assessment of the quality of existing and widely used satellite-based products (such as CS-2 and CryoSat-2/SMOS - herein and further CS-2/SMOS - ice thickness data sets) utilized in polar climate studies for different seasons. This assessment will be achieved through a comparison of those products with Upward-Looking Sonar (ULS) observations collected at a mooring in the eastern Arctic Ocean.

2. Materials and Methods

2.1. Upward-Looking Sonar and Oceanographic Measurements

In this study, we used ULS observations at the mooring deployed in September of 2013 at the northern slope of the Laptev Sea (78°25'N, 125°04'E) as a part of the Nansen and Amundsen Basins Observational System (NABOS) program (see **Figure 1** for mooring location; [7]) and recovered after two years in September of 2015. The mooring, referred to as the M1-4 mooring, was outfitted with an acoustic Ice Profiling Sonar (IPS; the same as ULS) produced by ASL Environmental Sciences. The ULS was designed to achieve accurate sea ice draft measurements with a manufacturer specified accuracy of approximately 5 cm. The ULS sampling rate at the mooring was set to 20 seconds, enabling successful resolution of the spatial structure of large ice keels above the instrument. The sea ice draft measurements were accompanied by CTD (conductivity-temperature-depth) records in the upper ocean layer, carried out using an SBE-37 instrument (Sea-Bird Electronics Inc) deployed at the same depth level (~50 m) as the ULS. Accuracies of temperature and salinity registration with this instrument are 0.001°C and 0.003 psu, respectively.

2.2. Satellite-Based Ice Thickness

For comparison we used ice thicknesses at the mooring site retrieved from the CS-2 satellite mission operated by the European Space Agency. CS-2 radar altimeter measures surface elevations of sea ice floes and open ocean leads, providing estimates of sea ice freeboard (the height of sea ice above the water surface). A calculation of ice thickness from freeboard measurements was performed assuming that the sea ice floats in a hydrostatic equilibrium [8–11] and using snow loads derived from the climatology snow distribution (EWG, 1998). The raw CS-2 altimeter data were processed at Alfred Wegener Institute (Kiel, Germany) and available from http://data.seaiceportal.de website on a regular 50-km grid, covering the Arctic Ocean limited by the 88°N latitude, with a bi-weekly temporal resolution.

The uncertainties in sea ice thickness stemming from the method based on ice freeboard measurements are notably pronounced, particularly when dealing with thin ice, as indicated in [12]. To enhance the accuracy of ice thickness estimates during the ice formation stage, we augmented our analysis with data from the Soil Moisture and Ocean Salinity (SMOS) dataset. This dataset estimates sea ice thickness using surface brightness temperatures measured by the satellite-based Microwave Imaging Radiometer at 1.4 GHz frequency in full polarization [13–15]. While the radiometer-based approach becomes less sensitive for thick ice (>1 m), the relative uncertainties for thin ice are significantly smaller compared to those observed with altimetry-based retrievals (see [10] and the references therein for more details). The original SMOS footprint varies from ~35 to ~50 km, depending on the satellite trajectories, enabling replication of the regular 50-km grid used in the CS-2 dataset. The SMOS and merged CS-2/SMOS ice thickness products used in our studies, along with details of satellite data processing, can be accessed from the website icdc.cen.uni-hamburg.de.

Preprints (www.preprints.org) | NOT PEER-REVIEWED | Posted: 2 August 2023 doi:10.20944/preprints202308.0112.v1

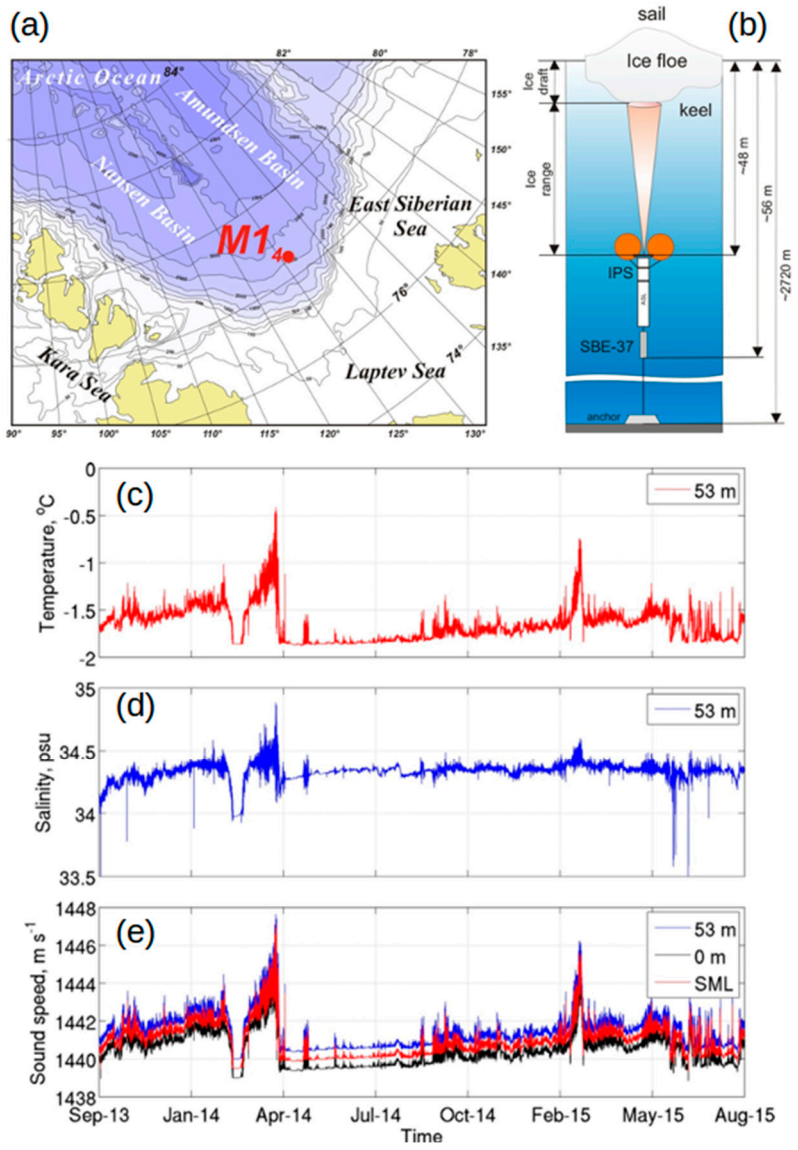

Figure 1. (**a**) Position of the M1-4 mooring at the slope of the Laptev Sea in 2013-2015 and (**b**) schematics of the upper part of the deployed mooring. Time series of temperature (**c**), salinity (**d**), and speed of sound (**e**) in the upper ocean layer at M1-4 mooring in 2013-2015. The sound speed at 0-m level depth and in the surface mixed layer (SML) was calculated assuming uniform temperature and salinity distributions within the mixed layer.

2.3. Sea Ice Concentrations and Drift Velocities

For deeper insight at ice state around the mooring site and in the eastern EB we complemented ice thickness observations by daily SMMR-SSM/I-SSMIS satellite-based ice concentrations (NASA team algorithm; accessible from ftp://sidads.colorado.edu/pub/DATASETS/nsidc0051_gsfc_nasateam_seaice/). This dataset is available on a 25-km polar stereographic grid for the entire Arctic Ocean, so we interpolated ice concentrations at the position of the M1-4 mooring from the four nearest nodes in this dataset. Ice concentrations around the mooring were complimented by sea ice motion vectors retrieved from Polar Pathfinder mission with daily resolution and available from the National Snow and Ice Data Center (NSIDC, http://nsidc.org/data/NSIDC-0116/versions/3).

2.4. Snow Depth on Sea Ice

The hydrostatic approach used for the calculation of ice thickness from ice draft measurements requires knowledge of snow accumulation on the top sea ice. In this study we used climatologically

Preprints (www.preprints.org) | NOT PEER-REVIEWED | Posted: 2 August 2023 doi:10.20944/preprints202308.0112.v1

mean snow depths taken from the Environmental Working Group (EWG) meteorological atlas of the Arctic (available from the http://nsidc.org/data/g01938 website) interpolated from a regular grid to the site of M1-4 mooring. Since the atlas utilizes snow depth and density measured at Soviet drifting stations in 1954–1991 - over than two decades before the mooring deployment, we concurrent the EWG climatological snow depth with snow measurements collected at the nearest to the mooring site meteorological station in Tiksi in 2013-2015 for comparison (**Figure 2a**). The collected snow measurements at Tiksi station includes regular measurements of snow thicknesses with daily (for thin <0.2-m ice) and ten-day (for thick >1-m ice) temporal resolutions [16]. Recognizing the natural heterogeneities of snow cover, the average error of these measurements can be estimated as 0.5 cm.

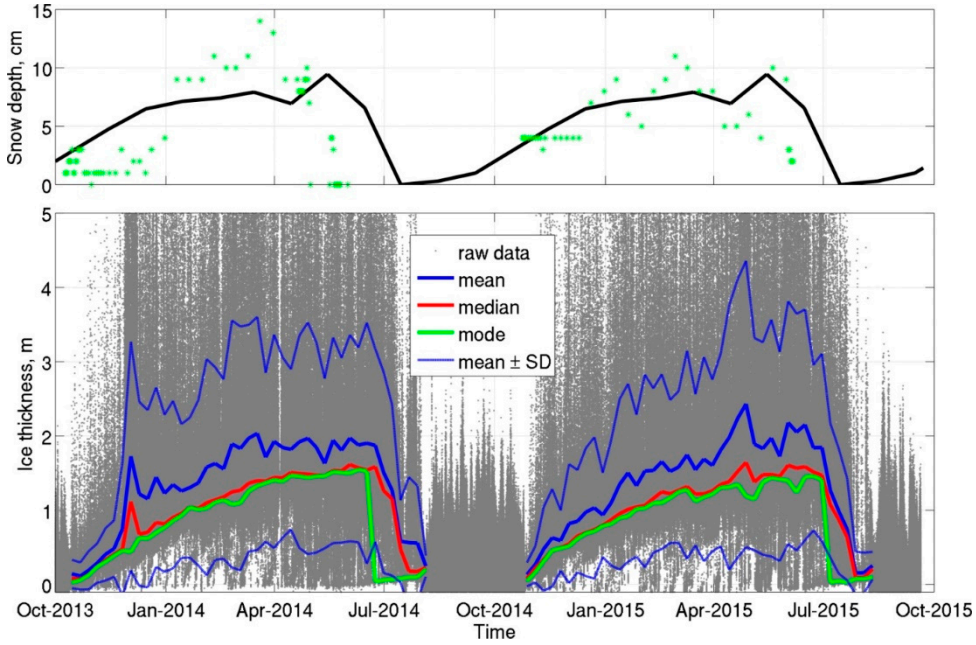

Figure 2. (**a**) Climatological snow depth (in cm) on the surface of sea ice at the M1-4 mooring site, located at the Laptev Sea slope, during the period of 2013-2015 as recorded by the EWG. In panel (**a**), the green stars indicate the snow depths measured at the Tiksi meteorological station from 2013 to 2015. Figure (**b**) displays the sea ice thickness measured by the Upward-Looking Sonar at the M1-4 mooring site during the same period, represented as grey dots. Note that the actual range of ice thicknesses (from 0.03 to ~24 m) was limited to 5 m for better visualization. Ice thickness statistics (means, medians, modes, and standard deviations; color curves) were calculated using a bi-weekly running window.

3. Results

3.1. ULS Record Processing

To accomplish the objective of this study, we meticulously processed the available ULS record obtained from the mooring site spanning the years 2013 to 2015. For the ice sonar data processing, we utilized the ASL Environmental Sciences Processing Toolbox package, specifically designed for this task by the ULS instrument manufacturer. This toolbox has a successful track record of processing numerous ULS records from various regions of the Arctic Ocean (e.g., [17–19] and others). The processing of the ULS data confirmed the high quality of the record obtained at the M1-4 mooring during 2013-2015, with no significant data gaps (see **Figure 2** for an example). Notably, the percentage of low-quality data within the ULS record from mooring M1-4 was less than 0.01% for the entire period of 2013-2015.

To enhance the precision of ice draft estimates obtained from the ULS acoustic echoes, several significant corrections have been implemented during the data processing. One notable correction involved adjusting the sound speed to account for variations in water density within the upper ocean layer, which represents a significant contributor to uncertainties in the ice thicknesses estimated from

Preprints (www.preprints.org) | NOT PEER-REVIEWED | Posted: 2 August 2023 doi:10.20944/preprints202308.0112.v1

acoustic sonar data [17]. For this purpose, temperature and salinity measurements taken in the upper ocean (**Figure 1c–e**) were utilized to calculate the speed of sound at the mooring location. To address the lack of temperature and salinity data near the ice base, we followed the approach proposed by Pickart et al. [20], extrapolating observations from the CTD instrument upward throughout the entire mixed layer and assuming a vertically-uniform distribution of temperature and salinity within this layer.

In order to account for variations in atmospheric sea-level pressure at the mooring, additional adjustments were applied to the ULS "pseudo" ice drafts. These adjustments were necessary as changes in atmospheric pressure can impact the depth estimates derived from the instrument's hydrostatic pressure measurements. To perform this correction, we utilized the 6-hour output data from the Era-Interim reanalysis model (available from https://www.ecmwf.int/en/forecasts/dataset/ecmwf-reanalysis-interim). The simulated sea-level pressure was then interpolated to the specific position of the mooring, covering the time span from September 2013 through September 2015.

In the final step, the initial high-resolution time series of ice thicknesses (at 20-second intervals) was averaged over daily, bi-weekly, and monthly periods to align with the resolution of the CS-2 and CS-2/SMOS datasets used for statistical analysis and evaluation in this study. Additionally, a spatial series of ice thicknesses was generated by interpolating ice velocity measurements to precisely match the location of the M1-4 mooring, using the temporal ice thickness record. The comparison between this spatial series and the temporal series facilitated an assessment of any potential influence of ice advection on the distribution of sea ice thickness. Although the probability distribution functions (not shown) for both records exhibited moderate differences, for our purposes, we can focus solely on the temporal ice thickness series. After careful processing and quality control, a two-year-long series of ice draft/thickness from this mooring became available for analysis.

3.2. Sesonal Evolution of Sea Ice Thickness

The ULS record from the M1-4 mooring captures two year-long cycles of seasonal sea ice evolution in the eastern EB. Ice draft measurements suggest that the beginning of ice formation, estimated as a steady increase of daily ice thickness, occurs in mid-October for both years (**Figure 2b**), with insignificant differences in four days between 2013 and 2014 due to differences in the atmospheric radiative forcing. Sea ice reaches its maximum development at the end of May or in the beginning of June, when its modal thickness was close to 1.5 m (Table 1). At the same time, the maximum modal thicknesses in the 2014-2015 season turned out to be 8 cm less, compared to those observed in 2013-2014 season. The curve of the seasonal ice thickness variations is significantly asymmetric. Active melting of sea ice in the area of mooring deployment begins in mid-June and continues for 1.5-2 months in such a way that by early August the area under study becomes ice-free. At the same time, the beginning of active ice melting is consistent with the dynamics of snow cover at the nearby Tiksi meteorological station, at which the most dramatic reduction in the modal ice thickness was observed only after the snow had completely melted (**Figure 2**).

Table 1. The basic statistics of sea ice thickness derived from the ULS record collected at the M1-4 mooring site during the period of 2013-2015.

Year / Month	2013-14					2014-15				
	Mean, m	Std, m	Median, m	Mode, m	Max, m	Mean, m	Std, m	Median, m	Mode, m	Max, m
September	0.30	0.26	0.26	0.20	16.35	0.32	0.21	0.28	0.24	2.06
October	0.17	0.19	0.12	0.10	4.72	0.20	0.17	0.13	0.08	1.75
November	0.51	0.62	0.37	0.28	10.98	0.54	0.53	0.43	0.44	10.08
December	1.30	1.26	0.72	0.66	16.25	0.98	0.82	0.74	0.72	12.18
January	1.28	1.02	0.95	0.88	16.75	1.40	1.03	1.06	1.00	16.79
February	1.61	1.41	1.13	1.02	19.05	1.60	1.09	1.26	1.16	17.75

 doi:10.20944/preprints202308.0112.v1

March	1.86	1.47	1.33	1.30	19.21	1.69	1.24	1.30	1.24	23.48
April	1.87	1.32	1.45	1.40	18.48	2.08	1.70	1.45	1.34	18.62
May	1.78	1.32	1.46	1.42	18.29	1.85	1.48	1.46	1.42	20.23
June	1.90	1.41	1.54	1.50	15.88	2.01	1.43	1.53	1.42	17.35
July	0.83	0.96	0.63	0.04	21.83	0.89	0.87	0.82	0.04	12.52
August	0.19	0.12	0.17	0.08	1.07	0.18	0.23	0.12	0.04	7.45

Starting from December, the sea ice thickness demonstrates large variability so that its monthly standard deviations (SD) become comparable to the mean thickness of the grown sea ice (Table 1).

3.3. Sea Ice Keels

One of the advantages of using acoustic ice sonars in studying sea ice is the possibility to examine the distribution and spatial structure of ice keels, which is practically impossible when using satellite-based ice thicknesses. For the assessment of ice keel depth extrema, we calculated the maxima of sea ice thickness for each month of the year, summarized in Table 1. The ULS ice draft record in 2013-15 showed that deep ice keels are evident in the eastern EB during the entire season of ice growth and melting (Table 1). As an example, the mooring recorded an absolute maximum depth of hummock keels, reaching approximately 23.5 meters, near the conclusion of the ice growth season in March 2015. However, a comparable ice keel depth was observed during the melting season in July 2014, when ice keels reached ~22 m depth. Comparable ice keel depths were also registered in other months except for September and October when the locally grown sea ice, likely, was too thin to form substantial hammocks. The horizontal scale of the continuous ridged ice areas, estimated using ice drift velocities, varied from tens of meters to several kilometers. Most likely, such a significant range is due to an arbitrary orientation of the ice deformation axes to the direction of the predominant ice drift at the mooring.

3.4. CS-2, CS-2/SMOS, and ULS Ice Thickness Comparison

The processed series of sea ice thicknesses at the M1-4 mooring from 2013 to 2015 offers a rare and valuable opportunity to validate satellite-based ice products available for the eastern EB of the Arctic Ocean. As a rule, this region faces limited long term in-situ observations due to challenging ice and weather conditions. The retrieved CS-2 and CS-2/SMOS ice thicknesses alongside those from the ULS instrument were used to calculate bi-weekly and monthly statistics (e.g., means, medians, modes, and standard deviations; **Figure 3**). Additionally, we assessed biases and established a linear best-fit relationship between the CS-2, CS-2/SMOS, and ULS ice thicknesses to quantify potential discrepancies between remotely sensed and in-situ ice thickness measurements in the eastern EB. This analysis aims to offer a possible approach for correcting the remotely sensed observations. However, it's worth noting that satellite products like CS-2 and the merged CS-2/SMOS dataset have limited measurements of thin ice (<0.5 m). Consequently, the comparison of these data with ULS measurements at M1-4 moorings may introduce significant uncertainties.

Preprints (www.preprints.org) | NOT PEER-REVIEWED | Posted: 2 August 2023 doi:10.20944/preprints202308.0112.v1

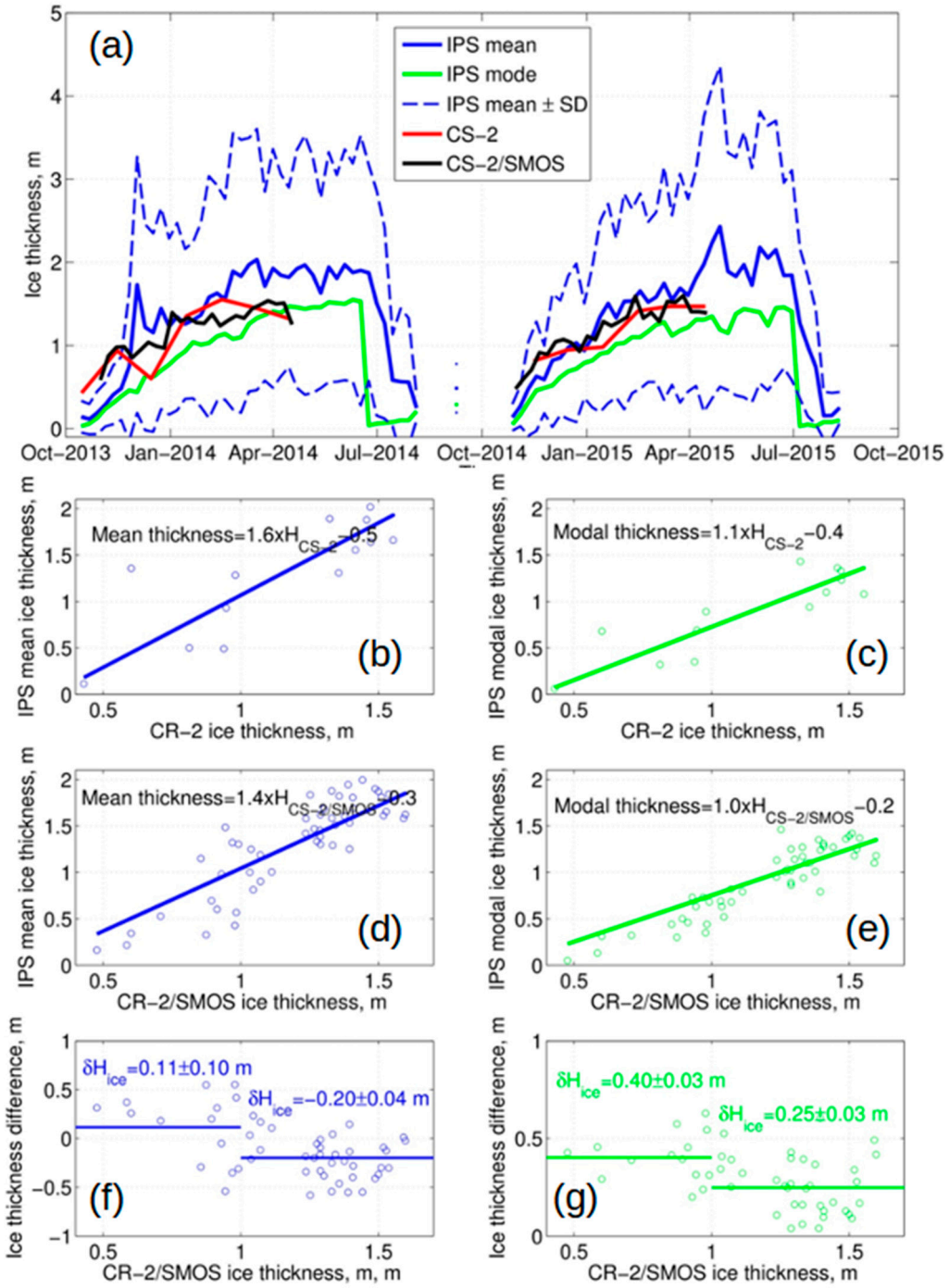

Figure 3. The sea ice thickness data obtained using the CS-2 and CS-2/SMOS datasets supplemented by the IPS-based thickness measurements taken at the M1-4 mooring site during the period of 2013-2015. The lack of ULS-based ice measurements from August to mid-October indicates an open water period.

We note that the satellite-based ice thicknesses series successfully captured all essential features of seasonal variations of ice at the mooring and agree well with seasonal ice changes reproduced by ice sonar observations (**Figure 3**). In line with this good agreement for both the CS-2 and CS-2/SMOS ice products, the determination coefficient (R^2) between the best fit lines of the ULS- and satellite-based ice thickness are high and varies from 0.88±0.20 for the modal ice thickness for the CS-2/SMOS dataset to 0.92±0.21 for the median ice thickness. The calculated regression equations (**Figure 3b–e**) provide us with the most easy-to-use opportunity to correct both satellite-based ice products and get better correspondence with the instrumental observations of ice thickness in that region. However,

 doi:10.20944/preprints202308.0112.v1

despite the high correlation, CS-2 and CS-2/SMOS ice thicknesses are biased compared to the ULS observations. This bias is evident for all seasons and insensitive to which statistics (mean or modal ice thickness) we used for the comparison. To further investigate these biases in greater detail, we conducted a separate comparison of ice thickness for two distinct periods: when sea ice has the moderate (<1m) and thick (>1m) ice thickness. This analysis allowed us to assess how various properties of the ice cover, such as surface emissivity, freeboard height, snow cover, and others, might potentially contribute to these differences. The comparison of key statistical parameters revealed that both satellite products (CS-2 and CS2/SMOS) exhibit substantial overestimations (up to 40 cm) in sea ice thickness for both moderate and thick ice conditions when compared with the ULS modal ice thickness. Consequently, it is likely that these satellite products cannot be used without some form of bias correction (as depicted in Figure 3g). At the same time, a systematic bias for the mean values of sea ice thickness is not as big (~20 cm), but also significant. The young ice forms observed at the M1-4 mooring site during November-December pose challenges for detection using the satellite-based ice products utilized. The discrepancies between these products for thin ice were generally larger compared to thick ice (up to 50 cm); however, the statistical robustness for these differences was lower. This implies that a more sophisticated correction of the satellite product might be necessary to achieve better matching with in-situ observations during the early stages of the ice growth.

4. Discussion

4.1. Sea Ice Ridging

In the previous section, we described the substantial (up to 40 cm) bias evident for the modal and mean ice thickness between the satellite-based ice thickness products and in-situ ULS observations. The reasons for this bias may be manifold and include both the technical features of the satellite sensors used as well as the natural variability of sea ice cover. One of the potentially important contributors to this bias is the sea ice thickness variability due to ice ridging, which is not sufficiently reproduced by satellite imagery with the relatively coarse spatial resolution but captured by our ULS pobservations.

To evaluate the impact of ice deformation (ridging) on sea ice thickness as measured by the ice sonar at the mooring, we conducted separate statistical analyses for both level (undeformed) and ridged ice on monthly basis. To differentiate between these two ice types, we applied the criterion proposed by Melling and Riedel [17] for the Beaufort Sea. As per this criterion, the draft of level ice should exhibit variations of less than 0.25 meters over ice segments of 10 meters in length. It is important to note that this criterion might not be applicable during the summer months (June-August) – the period of strong ice melting - because substantial pressure ridging is unlikely to occur under conditions of large areas of open water. As a result, the increased sea ice variability observed in summer is more likely a reflection of natural heterogeneity in melted ice rather than ice ridging.

Tables 2 and 3 provide an overview of the basic statistical properties of sea ice thickness estimated separetely for both level and ridged ice types. Analysis of the collected 2013-2015 ULS record indicates a prevalence of ridged ice over level ice at the continental slope of the Laptev Sea, highlighting the significant role of ice dynamics as a mechanism of the formation of sea ice cover in the EB of the Arctic Ocean. The occurrence of ridged ice was most pronounced during spring months (from March through May), with this ice type being observed approximately 60% of the time, compared to around 40% for level ice. Notably, the most substantial relative contribution of ridging to ice thickness was observed during the early ice formation period (October-December) for thin (<1 m) ice, when the relative difference between the mean and modal ice thicknesses – an average mesure of variations between the deformed and thermodynamically grown sea ice - could be as high as 70%. This period coincedes with the period when the radar altimeter-based products like CS-2 has large uncertanty which makes the use of this sattelite product even more difficult.

Preprints (www.preprints.org) | NOT PEER-REVIEWED | Posted: 2 August 2023 doi:10.20944/preprints202308.0112.v1

Table 2. Basic ice thickness statistics for level sea ice derived from the ULS observations at M1-4 mooring during 2013-2015.

Year / Month	2013-14					2014-15				
	Mean, m	Std, m	Median, m	Mode, m	Occurrence, %	Mean, m	Std, m	Median, m	Mode, m	Occurrence, %
September	0.20	0.08	0.20	0.24	47	0.22	0.10	0.21	0.18	29
October	0.12	0.06	0.11	0.10	61	0.10	0.05	0.09	0.08	40
November	0.34	0.12	0.34	0.28	70	0.39	0.13	0.39	0.34	68
December	0.64	0.24	0.63	0.66	43	0.71	0.14	0.71	0.72	59
January	0.90	0.18	0.90	0.88	56	1.02	0.25	1.01	1.00	59
February	1.05	0.25	1.04	1.02	46	1.19	0.22	1.19	1.16	48
March	1.22	0.30	1.26	1.30	41	1.24	0.21	1.25	1.24	50
April	1.36	0.25	1.40	1.42	41	1.30	0.46	1.34	1.34	45
May	1.31	0.41	1.43	1.42	48	1.14	0.50	1.32	1.42	40
June	1.29	0.49	1.46	1.50	40	1.39	0.28	1.43	1.42	36
July	0.49	0.45	0.40	0.04	55	0.48	0.44	0.43	0.04	50
August	0.13	0.06	0.12	0.08	31	0.09	0.06	0.07	0.04	57

Table 3. The same as in Table 2 but for ridged ice.

Year / Month	2013-14					2014-15				
	Mean, m	Std, m	Median, m	Mode, m	Occurrence, %	Mean, m	Std, m	Median, m	Mode, m	Occurrence, %
September	0.45	0.34	0.37	0.18	53	0.50	0.36	0.41	0.24	71
October	0.33	0.29	0.24	0.12	39	0.40	0.29	0.34	0.14	60
November	0.87	1.00	0.50	0.34	30	0.83	0.82	0.54	0.44	32
December	1.75	1.47	1.20	0.62	57	1.35	1.16	0.90	0.72	41
January	1.73	1.37	1.20	0.98	44	1.90	1.40	1.36	1.00	41
February	2.06	1.75	1.36	1.02	54	1.94	1.37	1.41	1.16	52
March	2.25	1.74	1.56	1.26	59	2.09	1.60	1.49	1.24	50
April	2.14	1.56	1.57	1.40	59	2.66	2.02	1.89	1.34	55
May	2.14	1.62	1.60	1.42	52	2.26	1.68	1.71	1.40	60
June	2.22	1.62	1.72	1.50	60	2.28	1.63	1.72	1.44	64
July	1.15	1.20	0.89	0.04	45	1.22	0.99	1.03	0.04	50
August	0.36	0.28	0.29	0.14	69	0.46	0.40	0.34	0.18	57

4.2. Sources of Ice Formation in the Easdtern EB

Despite valuable advantages, long-term measurements of sea ice employing ice profiling sonars are still rare, significantly reducing the possibility of an extended comparison. However, our conclusions about the discreapncy between the CS-2, CS-2/SMOS and ice sonar observations made for the mooring site at the Laptev Sea slope that can be considered from larger perspective. This seems to be reasonable assuming that the ice cover formation is not a strictly local process, but mostly distant one due to ice advection.

Figure 4 shows backward sea ice trajectories calculated using daily NSIDC sea ice velocities in 2013-2015. The reconstructed ice trajectories for both years suggest that the primary area of ice formation, which was subsequently being advected to the site of M1-4 mooring, was in the shallow shelf area of the Laptev Sea. These results confirm the essential role of the Laptev Sea shelf in establishing basin-wide sea ice conditions in the eastern Arctic in response to regional feedback in atmospheric and oceanic circulation (for example, see [21]). Since the statistical comparison between the satellite observations and in situ measurements of ice thicknesses discussed in this paper includes at least two complete seasonal cycles during which sea ice was advected from the Laptev Sea shelf to

Preprints (www.preprints.org) | NOT PEER-REVIEWED | Posted: 2 August 2023 doi:10.20944/preprints202308.0112.v1

the deep Eurasian Basin, we can reasonably assume that the conclusions about the significant discrepancies in ice thickness among the satellite-based products and instrumental observations are valid not only for the local area of M1-4 mooring but for more extended area of the southern part of the Laptev Sea.

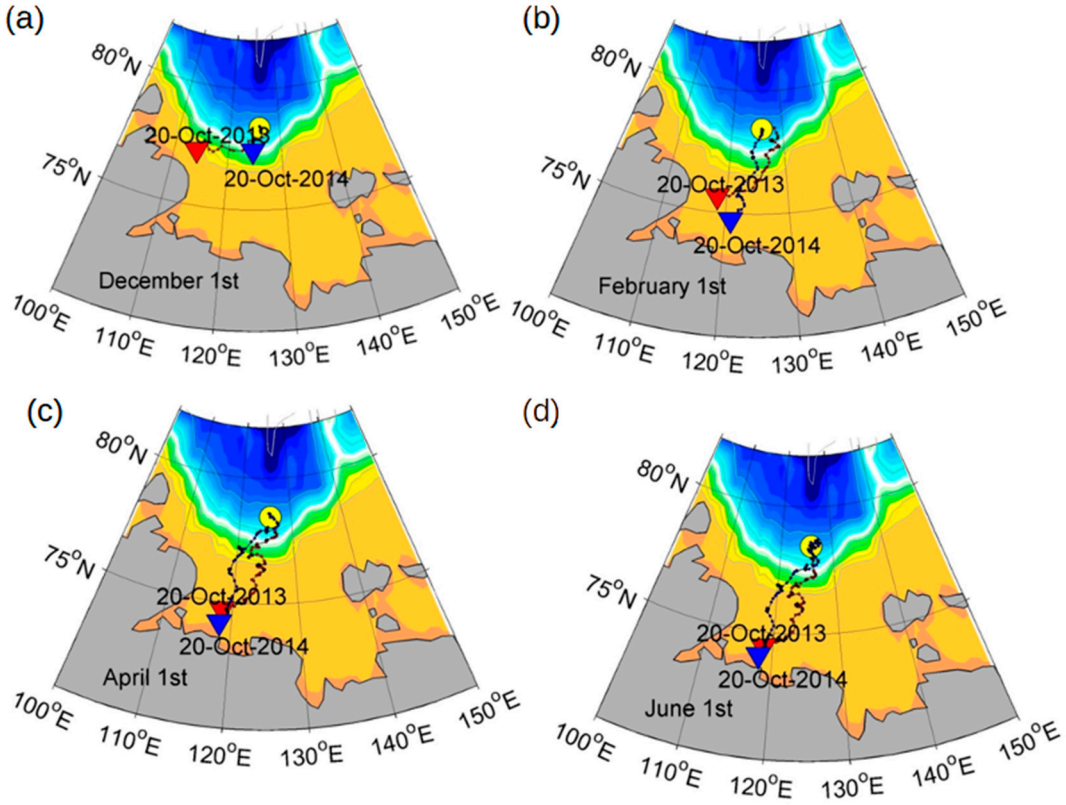

Figure 4. Backward sea ice trajectories in 2013-2015 calculated using daily NSIDC sea ice drift velocities. Red and blue triangles indicate locations of ice floes on 20 October 2013 and 2014, which were advected through the M1-4 mooring site on (**a**) 1st December, (**b**) 1st February, (**c**) 1st April, and (**d**) 1st June. Yellow circles show the position of M1-4 mooring.

5. Conclusions

In this study, we utilized upward-looking sonar observations from an oceanographic mooring installed at the northern slope of the Laptev Sea (78°25′N, 125°04′E) in September of 2013 alongside ice thickness data taken from the remotely sensed CryoSat-2 and CryoSat2/SMOS datasets. The comparison indicates that the satellite products used tend to significantly overestimate sea ice thickness (up to 40 cm) for both moderate and thick ice conditions, urging caution in their utilization. The most significant bias was found for the modal ice thickness – a measure of thermodynamically grown sea ice, so the discrepancy among the in-situ observations and remotely senced ice products may result in incorrect estimates of ice mass balance and its variability for the latter ones. Taking into account the wide implementation of satellite-based ice products for studies of in the Arctic Ocean sea ice changes and in the assimilation of ice thickness data in pan-Arctic ocean models, that positive biases may result in substantial underestimation for the rate of sea ice volume changes in the eastern EB in recent years reported in several studies (e.g., [3,22]).

Author Contributions: The study was carried out by AP, who also conducted the processing of ULS data and authored the manuscript.

Funding: This study was supported by NSF grant #1724523.

Data Availability Statement: The results of this study and original ULS data are available upon request to the author.

Acknowledgments: The ASL Environmental Sciences group (Canada) provided technical support and consultations for the execution of this study. The author also thanks Dr. Fukamachi (Arctic Research Center, Hokkaido University) for his valuable help and advice with the processing of ULS data and fruitful discussion of the results.

Conflicts of Interest: The author declares no conflict of interest.

References

1. Lindsay, R. and Schweiger, A., (2015): Arctic sea ice thickness loss determined using subsurface, aircraft, and satellite observations, *The Cryosphere*, 9, 269-283, doi:10.5194/tc-9-269-2015
2. Kwok, R. and N. Untersteiner, (2011): The thinning of Arctic sea ice, *Physics today*, April 2011, 36-41
3. Polyakov, I.V., Pnyushkov, A., Alkire, M., Ashik, I., Baumann, T., Carmack, E., Goszczko, I., Guthrie, J., Ivanov, V., Kanzow, T., Krishfield, R., Kwok, R., Sundfjord, A., Morison, J., Rember, R., Yulin, A., (2017) Greater role for Atlantic inflows on sea-ice loss in the Eurasian Basin of the Arctic Ocean. *Science*, 356(6335), 285-291, doi:10.1126/science.aai8204.
4. Tilling, R.L., Ridout, A., Shepherd, A., & Wingham D., J., (2015): Increased Arctic sea ice volume after anomalously low melting in 2013. Nature Geoscience, 8, 643–646, doi:10.1038/ngeo2489.
5. Kwok, R., and D. A. Rothrock, (2009): Decline in Arctic sea ice thickness from submarine and ICESat records: 1958 – 2008, Geophys. Res. Lett., 36, L15501, doi:10.1029/2009GL039035.
6. Kwok, R. (2018), Arctic sea ice thickness, volume, and multiyear ice coverage: Losses and coupled variability (1958 – 2018). Environ. Res. Lett. 13 (2018) 105005 https://doi.org/10.1088/1748-9326/aae3ec
7. Pnyushkov, A.V., and I.V. Polyakov, (2022): Nansen and Amundsen Basins Observational System (NABOS): Contributing to understanding changes in the Arctic. Oceanography, 35(1), https://doi.org/10.5670/oceanog.2022.104.
8. Laxon S. W., K. A. Giles, A. L. Ridout, D. J. Wingham, R. Willatt, R. Cullen, R. Kwok, A. Schweiger, J. Zhang, C. Haas, S. Hendricks, R. Krishfield, N. Kurtz, S. Farrell and M. Davidson, (2013): CryoSat-2 estimates of Arctic sea ice thickness and volume, Geophys. Res. Lett., 40, 732–737, doi:10.1002/grl.50193.
9. Ricker, R., Hendricks, S., Helm, V., Skourup, H., and Davidson, M.: Sensitivity of CryoSat-2 Arctic sea-ice freeboard and thickness on radar-waveform interpretation, The Cryosphere, 8, 1607–1622, doi:10.5194/tc-8-1607-2014, URL http://www.the-cryosphere.net/8/1607/2014/, 2014.
10. Ricker, R., Hendricks, S., Kaleschke, L., Tian-Kunze, X., King, J., and Haas, C. A.,: (2017) Weekly Arctic Sea-Ice Thickness Data Record from merged CryoSat-2 and SMOS Satellite Data, The Cryosphere Discuss., https://doi.org/10.5194/tc-2017-4.
11. Hendricks S., Ricker, R., Helm V., (2016): AWI CryoSat-2 Sea Ice Thickness Data Product (v1.2), User Guide., July 2016, available from http://data.meereisportal.de/data/cryosat2/doc/AWI_CryoSat2_Documentation_current.
12. Müller, F. L., Paul, S., Hendricks, S., and Dettmering, D.: Monitoring Arctic thin ice: a comparison between CryoSat-2 SAR altimetry data and MODIS thermal-infrared imagery, The Cryosphere, 17, 809–825, https://doi.org/10.5194/tc-17-809-2023, 2023.
13. Mecklenburg, S., Drusch, M., Kerr, Y., H., et al., (2012): ESA's Soil Moisture and Ocean Salinity mission: Mission performance and operations, IEEE Trans. Geosci. Remote Sens. 50 (5), pp. 1354-1366, doi: 10.1109/TGRS.2012.2187666.
14. Kaleschke, L., X. Tian-Kunze, N. Maaß, M. Mäkynen, and M. Drusch, (2012): Sea ice thickness retrieval from SMOS brightness temperatures during the Arctic freeze-up period, Geophys. Res. Lett., 39, L05501, doi:10.1029/2012GL050916.
15. Tian-Kunze, X.; Kaleschke, L.; Maaß, N.; Mäkynen, M.; Serra, N.; Drusch, M.; Krumpen, T., (2014): SMOS-derived thin sea ice thickness: Algorithm baseline, product specifications and initial verification. Cryosphere, 8, 997–1018.
16. Bogorodskii, P. V., Pnyushkov, A. V., Kustov, V. Yu., (2018): Seasonal freezing of a subwater ground layer at the Laptev sea shelf, In "The Ocean in Motion", Velarde, M.G., Tarakanov, R. Yu., Marchenko, A. V., (Eds.), Springer, 567 p.
17. Melling, H., P. H. Johnston, and D. A. Riedel, (1995): Measurement of the draft and topography of sea ice by moored subsea sonar, J. Atmos. Oceanic Technol., 12, 589-602.
18. Chave, R.A.J., D.D. Lemon, D.B. Fissel, (2004): Real-Time Measurement of Ice Draft and Velocity in the St. Lawrence. In: Proceedings of Oceans 2004 Conference, Kobe Japan, Nov. 10-12, IEEE Press. 5 p.

19. Hansen, E., et al. (2015): Time variability in the annual cycle of sea ice thickness in the Transpolar Drift. J. of Geophys. Res., 120(12): 8135-8150. doi: http://dx.doi.org/10.1002/2015JC011102.
20. Pickart, R. S., Spall, M., A., and Mathis, J., T., (2013): Dynamics of upwelling in the Alaskan Beaufort Sea and associated shelf–basin fluxes, Deep Sea Res., Part 1, 76 (10), 35–51.
21. Itkin, P. and Krumpen, T.: Winter sea ice export from the Laptev Sea preconditions the local summer sea ice cover and fast ice decay, The Cryosphere, 11, 2383–2391, https://doi.org/10.5194/tc-11-2383-2017, 2017.
22. Belter, H. J., Krumpen, T., von Albedyll, L., Alekseeva, T. A., Birnbaum, G., Frolov, S. V., Hendricks, S.,